The Influence of Steric Effects in Substituted 2,2′-Bipyridine on the Spin State of Iron(II) in $[FeN_6]^{2+}$ Systems

DJULIA ONGGO, JAMES M. HOOK, A. DAVID RAE* and HAROLD A. GOODWIN*
School of Chemistry, University of New South Wales, P.O. Box 1, Kensington, NSW 2033 (Australia)
(Received November 7, 1989)

Abstract

Tris(ligand)iron(II) complexes of 6-methyl-2,2′-bipyridine (mbpy) and 2-(pyridin-2-yl)quinoline (pyq) display anomalous magnetic properties which are associated with a temperature-induced singlet ($^1A_1$) ⇌ quintet ($^5T_2$) transition. Two forms of $[Fe(pyq)_3][ClO_4]_2$ were obtained: one which is essentially high spin over the range 89–300 K and the other which shows an almost complete, gradual transition in this range. In the three complex salts of $[Fe(mbpy)_3]^{2+}$ isolated, the perchlorate, fluoroborate and hexafluorophosphate, appreciable spin-pairing is observed at low temperatures but in no instance is the transition to singlet state species complete at 89 K. Data for solutions of both $[Fe(mbpy)_3][ClO_4]_2$ and $[Fe(pyq)_3][BF_4]_2$ indicate that negligible spin-pairing is observed down to 210 K. Mössbauer spectral data confirm the change in spin state populations in all solid salts and moreover indicate two sites for the high-spin species at low temperatures. It is believed that these may arise from ordering of anion sites in the lattice. In the room temperature structure of $[Fe(mbpy)_3][ClO_4]_2 \cdot \frac{1}{2}$mbpy disorder of one of the anions as well as the occluded free ligand occurs. In the structure of the complex cation considerable distortion is observed with the average Fe–N distance being 2.21 Å. The ligand molecules are not planar, the pyridyl rings being twisted 4.3, 16.4 and 17.8° about the inter-ligand bridge. The methyl substituent induces a steric barrier to coordination and also greater inter-ligand repulsions than in complexes of bpy and this is presumably responsible for the accessibility of the quintet state for Fe(II). The steric effects of the fused benzene ring in pyq are predicted to be similar. $[Fe(mbpy)_3][ClO_4]_2 \cdot \frac{1}{2}$mbpy crystallises in space group $P2_1/c$ ($Z = 4$) with cell parameters a = 19.769(10), b = 13.186(4), c = 15.043(8) Å. A total of 2509 reflections with $I_o > 3\sigma(I_o)$ were observed and gave a final R = 0.057.

Introduction

The effect of incorporation of a methyl group into the 2-position of 1,10-phenanthroline on the properties of the tris(ligand) iron(II) complex has been well documented. It has been found that the thermodynamic stability of the system is much reduced, compared to that of the corresponding complex of unsubstituted phenanthroline [1] and in addition there is a fundamental difference in the ground state of iron in the $[FeN_6]^{2+}$ complexes. Thus salts of $[Fe(mephen)_3]^{2+}$ (mephen = 2-methyl-1,10-phenanthroline) are high spin at room temperature, while those of $[Fe(phen)_3]^{2+}$ are low spin. At low temperatures, however, a generally incomplete transition to low-spin species is observed for the former salts, both in the solid state [2–5] and in solution [6]. This difference in behaviour has been generally ascribed to the weakening of the iron–nitrogen interactions by the steric effect of the substituent adjacent to a donor atom. The crystal structure of $[Fe(mephen)_3][BPh_4]_2$ does indeed reveal a strong steric influence of the methyl substituent [7]. Thus the average Fe–N distance (2.21 Å) is much longer than that in $[Fe(phen)_3]^{2+}$ (1.97 Å) [8], reflecting the effects of the different spin states [9] but the $Fe-N_{C-Me}$ distances (average 2.25 Å) are significantly greater than the $Fe-N_{C-H}$ (average 2.17 Å). Inter-ligand interactions, reinforced by the methyl substituents, influence the trigonal twist angles of the ligands as well as causing the cation to adopt the *mer* configuration. The ligand molecules remain fairly planar as is to be expected for the essentially rigid phenanthroline moiety. In 6-methyl-2,2′-bipyridine (mbpy) (**1**) the methyl group is similarly situated with respect to the donor atoms and can be expected to exert a similar influence on the metal–nitrogen interaction.

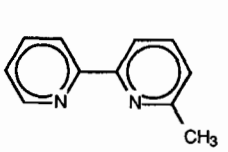

1

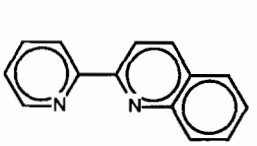

2

*Authors to whom correspondence should be addressed.

0020-1693/90/$3.50

The important structural difference between this molecule and 2-methyl-1,10-phenanthroline, however, is the relative lack of rigidity and the possibility of rotation about the C–C bridge. Because of this the properties of the $[Fe(mbpy)_3]^{2+}$ complex assume particular interest. This is especially so since it has been shown that rotation about the C–C bridge in the $[FeN_6]^{2+}$ complex of 3,3′-dimethyl-bipyridine is very pronounced (approximately 35°) and this has an marked effect on the electronic properties of the complex, a temperature-induced singlet ($^1A_1$) ⇌ quintet ($^5T_2$) transition being induced [10]. It is thus of interest to ascertain if the inherent flexibility in the bipyridine moiety allows the steric effects of the methyl substituent in the $[FeN_6]^{2+}$ complex of **1** to be accommodated with a less profound influence on the electronic properties of iron than those of 2-methyl-1,10-phenanthroline.

Any steric influence of the methyl group in **1** on the structure of the $[FeN_6]^{2+}$ complex would be expected to be comparable to that of the fused benzene ring in 2-(pyridin-2-yl)-quinoline (pyq) (**2**). The $[FeN_6]^{2+}$ complex of **2** was described earlier by Harris and co-workers [11] and a small decrease observed in the magnetic moment at low temperatures was ascribed to the partial population of singlet state species. The decrease was comparable to that observed for the $[FeN_6]^{2+}$ complex of 2-chloro-phenanthroline and similarly ascribed to a population of a singlet state at low temperatures [12], but it was later shown that that complex remains totally in a quintet state even at 5 K [13, 14]. It was thus considered worthwhile to re-examine the $[FeN_6]^{2+}$ complex of **2** and to compare its properties with those of the complex of **1**.

Experimental

Preparation of Ligands

6-Methyl-2,2′-bipyridine (mbpy) was prepared by the action of methyl-lithium on bipyridine according to the method of Schmalzl and Summers [15].

2-(2-Pyridin-2-yl)quinoline (pyq) was prepared according to the method described by Harris *et al.* [11].

Preparation of Complexes

$[Fe(mbpy)_3]X_2$; $X = ClO_4, BF_4$

To a warm solution of free ligand (0.5 g) in ethanol (10 ml) was added a warm solution of iron(II) perchlorate or fluoroborate hexahydrate (0.35 or 0.26 g, respectively) under a nitrogen atmosphere. The yellow complex salt was induced to crystallise directly. The products were washed with a little ethanol and dried *in vacuo* over P_2O_5.

$[Fe(mbpy)_3][PF_6]_2$

A solution of mbpy (0.38 g) in ethanol (5 ml) was added to iron(II) chloride tetrahydrate (0.15 g) in water (8 ml) under a nitrogen atmosphere. The mixture was filtered and ammonium hexafluorophosphate solution was slowly added to the filtrate when orange crystals separated immediately. These were washed with a small volume of cold water and dried in vacuum over P_2O_5.

$[Fe(pyq)_3][ClO_4]_2$ (sample 1)

This was prepared by interaction of iron(II) perchlorate hexahydrate with pyq in acetone followed by trituration with benzene, as described by Harris *et al.* [11].

$[Fe(pyq)_3][ClO_4]_2$ (sample 2) and $[Fe(pyq)_3][BF_4]_2$

These complexes were prepared by interaction of the ligand (0.5 g) in warm ethanol (5 ml) and iron(II) tetrafluoroborate or perchlorate hexahydrate (0.17 g) in ethanol (5 ml) under a nitrogen atmosphere. The red–orange crystals obtained were filtered off, washed with small amount of ethanol and dried over P_2O_5 in vacuum.

$[NiL_3][ClO_4]_2$ (L = mbpy or pyq)

The complex was isolated from the reaction between free ligand with nickel(II) perchlorate hexahydrate in absolute ethanol in the molar ratio 3:1. The solid product crystallised immediately, was collected, washed with ethanol and dried in vacuum over P_2O_5.

Analytical data for the complexes confirmed their purity, see "Supplementary Material'.

Crystal Structure of $[Fe(mbpy)_3][ClO_4]_2 \cdot \frac{1}{2}$mbpy

Crystal data

Crystals of $[Fe(mbpy)_3][ClO_4]_2 \cdot \frac{1}{2}$mbpy were grown by slow recrystallisation of the product obtained by direct interaction of iron(II) perchlorate and the ligand in ethanol from hot water containing a few drops of acetone. The compound $Fe(C_{11}H_{10}N_2)_3(ClO_4)_2\ 0.5(C_{11}H_{10}N_2)$, molecular weight 850.5, crystallises in $P2_1/c$ ($Z = 4$); a = 19.769(10), b = 13.186(4), c = 15.043(8) Å, V = 3920(3) Å^3, β = 90.98°(3), D_o = 1.46 and D_c = 1.44 g cm^{-3}; T = 22 °C. Distances from crystal faces to an internal origin: (100) 0.06, (−100) 0.06, (110) 0.06, (−1−10) 0.07, (1−10) 0.09, (−110) 0.10, (−20−5) 0.10, (101) 0.12 mm.

Structure determination

The reflection data were measured with an Enraf-Nonius CAD-4 diffractometer in $\theta/2\theta$ scan mode using graphite monochromatised molybdenum radia-

tion (λ = 0.7107 Å). Data were corrected for absorption. Structure solution was by MULTAN80 [16] and RAELS87 [17] was used for least-squares refinement of the observed data. Of the 4776 unique reflections, 2509 were considered observed with $I_o > 3\sigma(I_o)$. A final value of $R = 0.057$ was obtained. Reflection weights used were $1/\sigma^2(F_o)$, with $\sigma(F_o)$ being derived from $[\sigma^2(I_o) + (0.04I_o)^2]^{1/2}$. The weighted residual is defined as $R_w = (\Sigma w(\Delta F)^2/\Sigma wF_o^2)^{1/2}$. Atomic scattering factors and anomalous dispersion parameters were from International Tables for X-ray Crystallography [18]. ORTEP-II [19] was used for the preparation of the structural diagrams and an IBM3090 computer was used for all calculations. The dimensions of the two rings of the disordered uncoordinated ligand molecule were constrained to be equal. The disordered perchlorate ion was refined with just sufficient complexity of parameters to describe adequately the ion, as verified by back Fourier Transform techniques. It was shown that the residual electron density in this region in the map was not significantly different from any other region after a model of equal perfectly tetrahedral ions of refinable bond length was applied. Relative occupancy, orientation and position were refined. A common TLX thermal parameterisation was also applied.

Spectra

Electronic spectra were recorded on a Zeiss PMQ II spectrophotometer equipped with a diffuse relectance accessory. Solid samples were spread on filter paper and calibrated against magnesium oxide. Low temperature spectra were obtained by using a special brass attachment with silica glass windows. The fitting was sealed and a stream of cold nitrogen gas was passed over the assembly to prevent condensation. The fitting was then placed in contact with the base of an insulated brass dewar filled with liquid nitrogen. Variable temperature measurements were made without re-mounting the sample.

Mössbauer spectra were recorded with a spectrometer utilising a Wissel drive unit and a Norland multichannel analyser. The source used was ^{57}Co in a Pd matrix. The temperature of the absorber was maintained to within $\pm 1^\circ$ in a custom made cryostat. The velocity was calibrated against iron foil and sodium nitroprusside. The isomer shifts quoted are relative to the midpoint of the iron spectrum. Parameters (see Table 2) were calculated from a least-squares fit of the experimental data to Lorentzian line shapes.

Magnetism

Magnetic data for solid samples were obtained from a Newport variable-temperature Gouy system. Data for $[FeL_3]X_2$ in solution were obtained by the Evans NMR method [20]. The data have been corrected for diamagnetism. Magnetic moments were calculated according to the relationship $\mu_{eff} = 798(\chi_M T)^{1/2}$ (SI units).

Results and Discussion

The ligand **1** has been known for some time and there have been several reports of its preparation [15, 21–24]. In the present work it was obtained by the reaction of methyl-lithium with bipyridine according to the method of Schmalzl and Summers [15]. The coordination chemistry of **1** has been examined only relatively briefly. The tris(ligand) complexes of ruthenium(II) and osmium(II) [24], a dichloro-bis(ligand) complex of nickel(II), a mixed ligand complex of cobalt(II) [23], mono(ligand) complexes of copper(I) [25] and palladium(II) [26] have been described. In the present work emphasis is placed on the electronic and structural properties of salts of $[Fe(mbpy)_3]^{2+}$.

Magnetism of Salts of $[Fe(mbpy)_3]^{2+}$ and $[Fe(pyq)_3]^{2+}$

The temperature dependence of the magnetism of three salts $[Fe(mbpy)_3]X_2$ (X = ClO_4, BF_4, PF_6) is detailed in Table 1 and illustrated in Fig. 1. In all instances there is a decrease in moment at low temperatures, though this is small for the hexafluorophosphate salt. The moments at high temperature are normal for iron(II) in the quintet ($^5T_2$) state and the decrease at low temperatures suggests a contribution from an increasing population of singlet ($^1A_1$) species. From the nature of the curves in Fig. 1 it is evident that the moment would continue to decrease at temperatures below the experimental limit of the temperature range. The behaviour of these salts is thus similar to that of salts of $[Fe(mephen)_3]^{2+}$ but the quintet → singlet transition is centred at lower temperatures.

In their original report of the properties of $[Fe(pyq)_3][ClO_4]_2$ Harris and co-workers [11] obtained the complex from an acetone/benzene mixture and observed a very small decrease in magnetic moment at low temperatures. We have repeated this preparation and the magnetism of our sample (sample 1, Table 1, Fig. 1) almost reproduces that already reported. In the early report [11] the interaction of 2 and iron(II) perchlorate in ethanol apparently resulted in a bis(ligand) complex, but we have found that a tris(ligand) complex is readily isolable from this reaction mixture and this shows magnetic behaviour quite different from that of the complex isolated from acetone/benzene. The magnetic moment of the ethanol product (sample 2) is very strongly temperature dependent (Table 1, Fig. 1) and is indicative of an almost complete, continuous singlet ($^1A_1$) ⇋ quintet ($^5T_2$) transition. A tris(ligand) complex

TABLE 1. Magnetic data for complexes

T (K)	$10^{10} \times \chi_M$ ($m^3\ mol^{-1}$)	μ_{eff} (BM)	T (K)	$10^{10} \times \chi_M$ ($m^3\ mol^{-1}$)	μ_{eff} (BM)
$[Fe(mbpy)_3][BF_4]_2$ (solid)					
89.1	3730	4.60	108.6	3220	4.71
127.6	2960	4.90	151.6	2720	5.12
176.3	2470	5.27	200.8	2270	5.39
225.4	2050	5.43	249.8	1860	5.44
275.0	1690	5.44	304.4	1530	5.44
$[Fe(mbpy)_3][PF_6]_2$ (solid)					
89.1	4440	5.02	127.6	3160	5.07
176.3	2410	5.20	225.4	1910	5.24
275.0	1560	5.22	304.4	1430	5.26
$[Fe(mbpy)_3][ClO_4]_2$ (solid)					
89	3450	4.42	108.6	3090	4.62
127.6	2790	4.76	151.6	2560	4.97
176.3	2400	5.18	200.8	2180	5.27
225.4	2010	5.36	249.8	1840	5.41
275.0	1670	5.40	298.7	1510	5.35
$[Fe(mbpy)_3][ClO_4]_2$ (acetone solution)					
200	2160	5.25	220	1980	5.27
240	1820	5.27	260	1670	5.26
280	1570	5.29	296	1490	5.30
$[Fe(pyq)_3[ClO_4]_2 \cdot H_2O$ (solid) (sample 1)					
89.1	4820	5.23	108.6	4110	5.33
127.6	3600	5.40	151.6	3050	5.42
176.3	2650	5.45	200.8	2350	5.47
225.4	2080	5.46	275.0	1710	5.47
299.4	1530	5.39			
$[Fe(pyq)_3][ClO_4]_2 \cdot H_2O$ (solid) (sample 2)					
85.6	550	1.73	89.1	580	1.81
108.6	520	1.90	127.6	550	2.11
146.8	687	2.53	156.5	870	2.94
166.4	1160	3.50	176.3	1540	4.15
186.1	1740	4.53	205.8	1820	4.88
225.4	1730	4.98	249.8	1590	5.03
275.0	1490	5.10	299.4	1360	5.09
313.0	1270	5.02			
$[Fe(pyq)_3][BF_4]_2 \cdot H_2O$ (solid)					
85.6	950	2.27	89.1	960	2.33
108.6	1030	2.66	118.1	1170	2.96
127.6	1310	3.26	137.2	1560	3.69
146.8	1910	4.22	156.5	2160	4.64
166.4	2310	4.94	176.3	2360	5.15
200.8	2180	5.28	225.4	1990	5.34
249.8	1800	5.34	275.0	1650	5.37
294.6	1530	5.35			
$[Fe(pyq)_3][BF_4]_2 \cdot H_2O$ (acetone solution)					
290	1480	5.22	270	1580	5.21
250	1710	5.21	230	1850	5.20
210	1970	5.13	195	2080	5.08

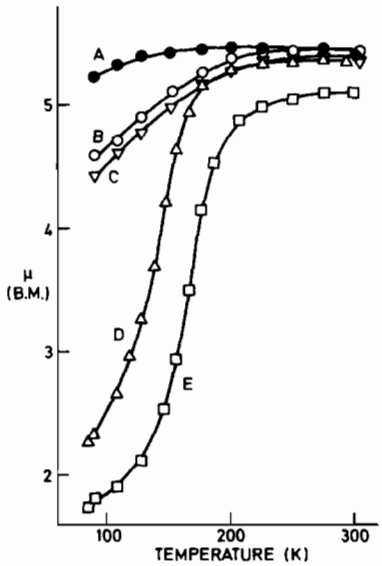

Fig. 1. Temperature dependence of the magnetic moment of: A, $[Fe(pyq)_3][ClO_4]_2$ (sample 1); B, $[Fe(mbpy)_3][BF_4]_2$; C, $[Fe(mbpy)_3][ClO_4]_2$; D, $[Fe(pyq)_3][BF_4]_2$; E, $[Fe(pyq)_3][ClO_4]_2$ (sample 2).

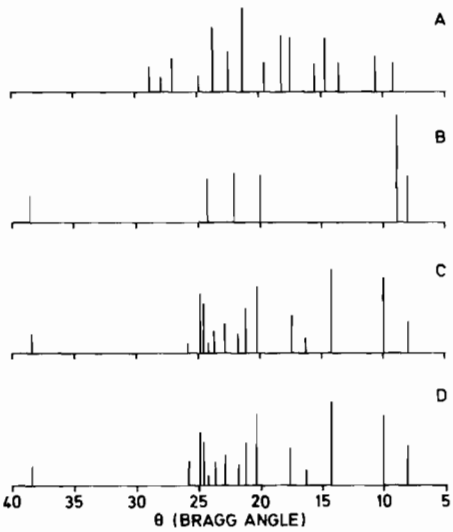

Fig. 2. X-ray powder diffraction profiles for: A, $[Fe(mpby)_3][ClO_4]_2$; B, $[Fe(pyq)_3][ClO_4]_2$ (sample 1); C, $[Fe(pyq)_3][ClO_4]_2$ (sample 2); D, $[Fe(pyq)_3][BF_4]_2$.

fluoroborate could also be isolated by interaction of the ligand with iron(II) fluoroborate in ethanol and the magnetism of this closely parallels that of the corresponding perchlorate. The two samples of the complex perchlorate represent different crystal modifications and the dependence of the detailed course of a spin transition in a crossover system on the nature of the particular crystal lattice has been long recognised [27]. That they are different in the present instance is revealed by their X-ray powder diffraction profiles, which are quite distinct (Fig. 2).

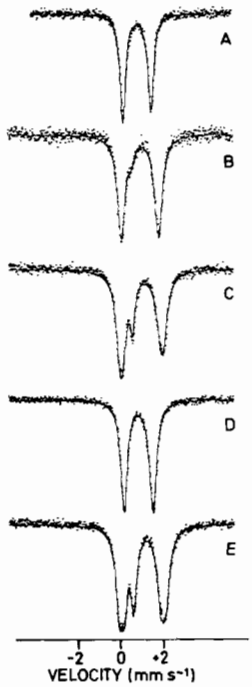

Fig. 3. Mössbauer spectra of: A, $[Fe(mbpy)_3][BF_4]_2$ at 298 K; B, $[Fe(mbpy)_3][BF_4]_2$ at 173 K; C, $[Fe(mbpy)_3][BF_4]_2$ at 77 K; D, $[Fe(mbpy)_3][ClO_4]_2$ at 298 K; E, $[Fe(mbpy)_3][ClO_4]_2$ at 77 K.

On the other hand the perchlorate sample 2 and the fluoroborate salt have very similar powder patterns, indicating that these salts are isostructural, and this is consistent with their similar magnetism. The possibility exists that the two samples of the complex perchlorate represent *fac* and *mer* isomers, though the facial isomer would not be expected to be favoured on steric grounds since it would lead to greater inter-ligand repulsions.

Magnetic data were obtained for both $[Fe(mbpy)_3][ClO_4]_2$ and $[Fe(pyq)_3][BF_4]_2$ in acetone solution (Table 1). Both complexes are essentially high spin within the experimental temperature range. The very small decrease observed for the moment of $[Fe(pyq)_3][BF_4]_2$ at the lowest temperature may reflect the onset of spin pairing since a change in colour of the solution is visible at this temperature (see below).

Mössbauer Spectra

The origin of the temperature dependence of the magnetism of salts of $[Fe(mbpy)_3]^{2+}$ is clearly revealed by Mössbauer spectral data. At room temperature the spectrum of the fluoroborate salt shows a single quadrupole split doublet (Fig. 3) with parameters (Table 2) normal for quintet state iron(II). The value for the quadrupole splitting is slightly greater than that observed [4, 5] for salts of $[Fe(mephen)_3]^{2+}$ but the isomer shift is almost

TABLE 2. Mössbauer spectral parameters

Compound	T (K)	Spin state	ΔE_Q[a] (mm s^{-1})	δ_{is}[a] (mm s^{-1})
$[Fe(mbpy)_3][BF_4]_2$	298	$^5T_2$	1.24	0.99
$[Fe(mbpy)_3][BF_4]_2$	173	$^5T_2$	1.60	1.11
$[Fe(mbpy)_3][BF_4]_2$	173	$^1A_1$	0.51	0.41
$[Fe(mbpy)_3][BF_4]_2$	77	$^5T_2$ (outer)	1.77	1.21
$[Fe(mbpy)_3][BF_4]_2$	77	$^5T_2$ (inner)	1.66	1.13
$[Fe(mbpy)_3][BF_4]_2$	77	$^1A_1$	0.73	0.38
$[Fe(mbpy)_3][ClO_4]_2$	298	$^5T_2$	1.28	0.99
$[Fe(mbpy)_3][ClO_4]_2$	77	$^5T_2$ (outer)	1.96	1.16
$[Fe(mbpy)_3][ClO_4]_2$	77	$^5T_2$ (inner)	1.52	1.16
$[Fe(mbpy)_3][ClO_4]_2$	77	$^1A_1$	0.72	0.40
$[Fe(pyq)_3][ClO_4]_2$ (sample 1)	298	$^5T_2$	1.49	0.97
$[Fe(pyq)_3][ClO_4]_2$ (sample 1)	77	$^5T_2$	1.60	1.13
$[Fe(pyq)_3][ClO_4]_2$ (sample 1)	77	$^1A_1$	0.73	0.49
$[Fe(pyq)_3][ClO_4]_2$ (sample 2)	298	$^5T_2$	1.30	1.00
$[Fe(pyq)_3][ClO_4]_2$ (sample 2)	77	$^5T_2$	2.33	1.14
$[Fe(pyq)_3][ClO_4]_2$ (sample 2)	77	$^1A_1$	0.76	0.46

[a]Estimated error ±0.03 mm s^{-1}.

the same. At lower temperatures the emergence of additional absorption becomes evident and this is due to a contribution from the singlet state species. At 173 K this appears principally as a shoulder on the low velocity line of the high-spin doublet but at 77 K it is clearly evident, one component of the doublet due to singlet state species overlapping with the low velocity line of the high-spin doublet. It is apparent that the major contribution to the spectrum at 77 K is from high-spin species, and this is consistent with the still relatively high value for the magnetic moment at 89 K. It is also evident from Fig. 3 that the lines due to the high-spin doublet become considerably broadened at low temperatures. This strongly suggests contributions from more than one high-spin species. This is perhaps even more marked in the low-temperature spectrum of the perchlorate where resolution into two high-spin doublets is almost visible. The origins of the broadening are not clear but a likely possibility is the occurrence of a disorder–order transition in the lattice sites for the anionic species. In the room temperature structure of $[Fe(mbpy)_3][ClO_4]_2 \cdot \frac{1}{2}$mbpy (see below) disorder in the anion orientation in the lattice has been detected and it is likely that this occurs in the Mössbauer sample too. While the structure at low temperatures has not been determined it is feasible that the anion orientations become ordered into two sites.

There is precedent for this behaviour. Indeed considerable line broadening was observed initially [3] for $[Fe(mephen)_3][ClO_4]_2$. Subsequently the lines were resolved by Fleisch and coworkers [5] into two separate doublets over the entire temperature range between 4.2 and 295 K. These were interpreted as arising from two different lattice sites for high-spin iron(II) characterised by a reversal of the orbital ground state in a trigonally distorted field, i.e. with ^5E and $^5A_1$ ground states. Order–disorder transitions have been directly detected by structural studies for anion orientations in the iron(II) spin crossover systems tris(2,2′-bi-2-imidazoline)iron(II) perchlorate [28] and tris(4-methyl-2(pyridin-2-yl)thiazole)iron(II) perchlorate [29] and for the former example a detailed analysis of the Mössbauer spectra below the disorder–order transition allowed resolution of two doublets due to high-spin iron(II). The line broadening effects observed were similar to those noted for salts of $[Fe(mbpy)_3]^{2+}$. Significant broadening has recently been reported for the high-spin lines in the spectrum of the $[FeN_6]^{2+}$ complexes of a series of pyridyltriazoles and again its origin in a disorder–order transition involving the anionic species was considered likely [30].

Mössbauer spectra for the two forms of $[Fe(pyq)_3][ClO_4]_2$ confirm the original proposal by Harris and co-workers [11] that this is a spin crossover system. For sample 1 the room temperature spectrum shows only a single doublet which has parameters normal for quintet state iron(II) but the spectrum at 77 K shows a very weak shoulder on the low-velocity component of the high-spin doublet (Fig. 4). This is clearly absent in the room temperature spectrum. Although parameters for this new absorption cannot be determined accurately it is evident that a relatively small value for both ΔE_q and δ_{is} is applicable (Table 2), consistent with its origins from a $^1A_1$ species. This is in accord with the slight decrease in the magnetic moment observed

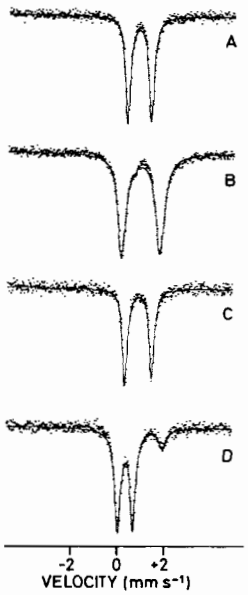

Fig. 4. Mössbauer spectra of: A, $[Fe(pyq)_3][ClO_4]_2$ (sample 1) at 298 K; B, $[Fe(pyq)_3][ClO_4]_2$ (sample 1) at 77 K; C, $[Fe(pyq)_3][ClO_4]_2$ (sample 2) at 298 K; D, $[Fe(pyq)_3][ClO_4]_2$ (sample 2) at 77 K.

at low temperatures. Again broadening is evident in the high-spin lines at low temperature but not to the exent observed in the spectra of the salts of $[Fe(mbpy)_3]^{2+}$ and the spectrum was fitted to a single quadrupole doublet for the quintet state species.

Mössbauer spectra for the sample of $[Fe(pyq)_3][ClO_4]_2$ prepared from ethanol (sample 2) clearly reveal the almost complete transition from quintet to singlet state species at low temperature, consistent with the magnetic data. The residual high-spin contribution at 77 K is responsible for the relatively weak, and somewhat broad line at high velocity (Fig. 4). The values for the quadrupole splitting for both forms of $[Fe(pyq)_3][ClO_4]_2$, whether in the singlet or quintet state, are in general greater than those for the salts of $[Fe(mbpy)_3]^{2+}$. This may be an effect of the more bulky substituent in **2** giving rise to somewhat greater distortion in the coordination environment about iron.

Electronic Spectra

In the solid state both $[Fe(mbpy)_3]X_2$ and $[Fe(pyq)_3][ClO_4]_2$ (sample 2) are strongly thermochromic. At room temperature $[Fe(mbpy)_3]X_2$ (X = ClO_4, BF_4) are light yellow, while both samples **1** and **2** of $[Fe(pyq)_3][ClO_4]_2$ are a light orange–red. At low temperatures $[Fe(mbpy)_3]X_2$ (X = ClO_4, BF_4] and $[Fe(pyq)_3][ClO_4]_2$ (sample 2) are deep red–violet. The visible change in colour is due essentially to a shift of the charge-transfer transition to lower energy at low temperature, together with a significant increase in its intensity (Fig. 5). The

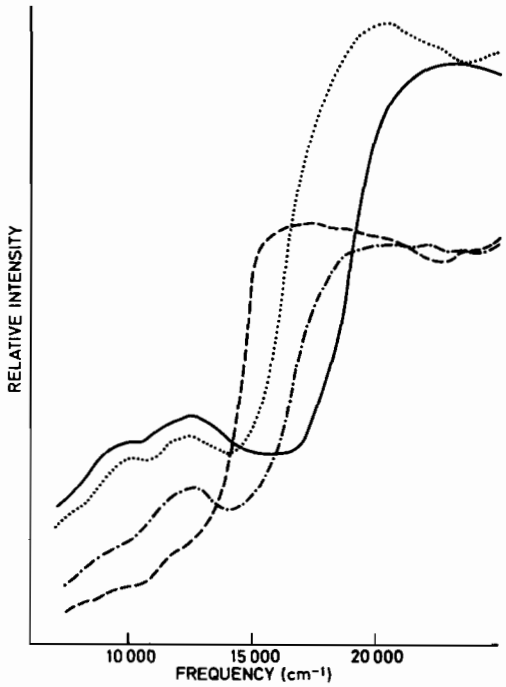

Fig. 5. Diffuse reflectance spectra of $[Fe(mbpy)_3][ClO_4]_2$ at 110 K (·····), $[Fe(mbpy)_3][ClO_4]_2$ at 298 K (——), $[Fe(pyq)_3][ClO_4]_2$ (sample 2) at 110 K (- - - -), $[Fe(pyq)_3][ClO_4]_2$ (sample 2) at 298 K (– · –).

spectra of complexes of both ligands also show ligand field absorption in the 12 000 cm^{-1} region. For $[Fe(mbpy)_3][ClO_4]_2$ this absorption is split, the principal component occurring at 12 400 cm^{-1} and a shoulder at 10 000 cm^{-1}, the splitting arising presumably from Jahn–Teller and/or low symmetry effects on the $^5T_{2g} \rightarrow {}^5E_g$ transition. The charge-transfer absorption extends to lower energy in the spectrum of $[Fe(pyq)_3][ClO_4]_2$. This is in accord with data obtained for the corresponding $[RuN_6]^{2+}$ complexes [24, 31]. Both samples of the iron complex also show ligand field absorption in the 12 000 cm^{-1} region, but it is centred at slightly lower energy (12 200 cm^{-1}) in sample 1 than in sample 2 (12 500 cm^{-1}). This is in accord with the relative favouring of spin pairing in sample 2. At low temperatures, the ligand field absorption becomes much less intense in all samples except sample 1 of $[Fe(pyq)_3][ClO_4]_2$. For this latter complex the absorption is found to be only slightly less intense but much less broad at low temperature. The spectral patterns are better resolved for spectra measured for solutions (Fig. 6) and the band positions are listed in Table 3. The iron complexes of both ligands are somewhat unstable to dissociation in solution and consistent values for the extinction coefficients could only be obtained in the presence of free ligand. No significant temperature dependence of the intensities of the bands was observed within the range of temperature available

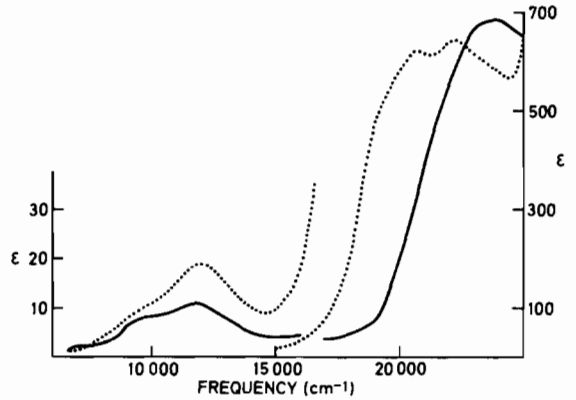

Fig. 6. Electronic spectra of $[Fe(mbpy)_3][ClO_4]_2$ (——) and $[Fe(pyq)_3][BF_4]_2$ (·····) in acetone solution.

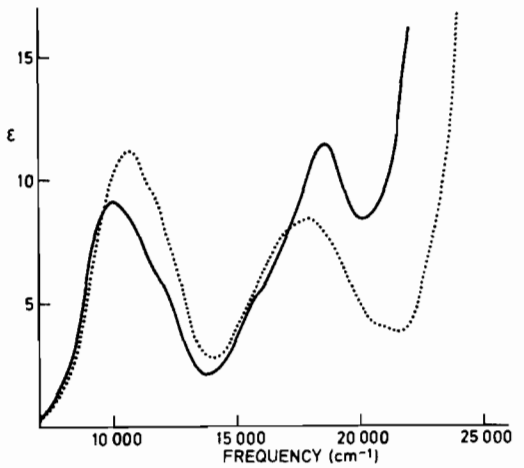

Fig. 7. Electronic spectra of $[Ni(pyq)_3][ClO_4]_2$ (——) and $[Ni(mbpy)_3][ClO_4]_2$ (·····) in acetone solution.

for measurements. However, the development of a significant red coloration was visible in the solution of $[Fe(pyq)_3][BF_4]_2$ at the lowest temperature reached in the measurement of magnetism in solution.

Nickel(II) complexes $[NiL_3][ClO_4]_2$ were also prepared so as to gain a reliable assessment of the relative field strengths of the ligands. These complexes are typical for nickel(II) derivatives of diimine ligand systems, having magnetic moments at 300 K of 3.03 (Curie–Weiss $\theta = 2°$) and 2.91 BM ($\theta = 22°$) for $[Ni(mbpy)_3][ClO_4]_2$ and $[Ni(pyq)_3][ClO_4]_2$, respectively. Their spectra show two well resolved ligand field bands due to the transitions $^3A_{2g} \rightarrow {}^3T_{2g}$ ($\nu_1 = 10Dq$) and $^3A_{2g} \rightarrow {}^3T_{1g}(\nu_2)$. In addition a shoulder is observed at about 12 000 cm^{-1} on the low energy band (Fig. 7), most likely associated with the spin forbidden $^3A_{2g} \rightarrow {}^1E_g$ transition [32]. It can be seen from the data in Table 3 that pyq provides a significantly weaker field ($Dq_{Ni^{2+}}$ = 1000 cm^{-1}) than mbpy ($Dq_{Ni^{2+}}$ = 1060 cm^{-1}), weaker in fact than that normally corresponding to the appearance of a spin transition in iron(II) [33]. Data were also obtained for $[Ni(mephen)_3][ClO_4]_2$ under the same conditions. For this $Dq_{Ni^{2+}}$ = 1100 cm^{-1} and this higher value is consistent with the greater tendency to spin pairing in salts of $[Fe(mephen)_3]^{2+}$ compared with salts of $[Fe(mbpy)_3]^{2+}$. $[Fe(mephen)_3]^{2+}$ shows broader and less well-defined absorption in the ligand field region than $[Fe(mbpy)_3]^{2+}$ due to the extension of the tail of the charge transfer absorption into this region, the maximum appearing at about 12 800 cm^{-1}.

Structure of $[Fe(mbpy)_3][ClO_4]_2 \cdot \frac{1}{2}mbpy$

Crystals of $[Fe(mbpy)_3][ClO_4]_2$ suitable for structure determination were grown from water containing a few drops of acetone. The actual crystal used contained half a molecule of free ligand per complex molecule in the lattice. The recrystallisation procedure thus obviously resulted in some decomposition of the complex.

A view of the complex cation and the atom labelling scheme are shown in Fig. 8. A view of the unit cell contents projected down *b* is shown in Fig. 9. Bond lengths are listed in Table 4, selected bond angles are given in Table 5 and fractional coordinates for non-hydrogen atoms are given in Table 6. The complex cation adopts a *mer* octahedral configu-

TABLE 3. Electronic spectral data

Complex	Solvent	ν (cm^{-1})	ϵ (l mol^{-1} cm^1)	Assignment
$[Fe(mbpy)_3][ClO_4]_2$	acetone	24000	700	$t_{2g} \rightarrow \pi^*$
$[Fe(mbpy)_3][ClO_4]_2$	acetone	11600	10.5	$^5T_{2g} \rightarrow {}^5E_g$
$[Fe(pyq)_3][ClO_4]_2$	acetone	20600	625	$t_{2g} \rightarrow \pi^*$
$[Fe(pyq)_3][ClO_4]_2$	acetone	22100	645	$t_{2g} \rightarrow \pi^*$
$[Fe(pyq)_3][ClO_4]_2$	acetone	12100	19	$^5T_{2g} \rightarrow {}^5E_g$
$[Ni(mbpy)_3][ClO_4]_2$	acetonitrile	10600	11.1	$^3A_{2g} \rightarrow {}^3T_{2g}$
$[Ni(mbpy)_3][ClO_4]_2$	acetonitrile	18000	8.4	$^3A_{2g} \rightarrow {}^3T_{1g}$
$[Ni(pyq)_3][ClO_4]_2$	acetonitrile	10000	8.6	$^3A_{2g} \rightarrow {}^3T_{2g}$
$[Ni(pyq)_3][ClO_4]_2$	acetonitrile	18600	11.4	$^3A_{2g} \rightarrow {}^3T_{1g}$
$[Ni(mephen)_3][ClO_4]_2$	acetonitrile	11000	12.5	$^3A_{2g} \rightarrow {}^3T_{2g}$

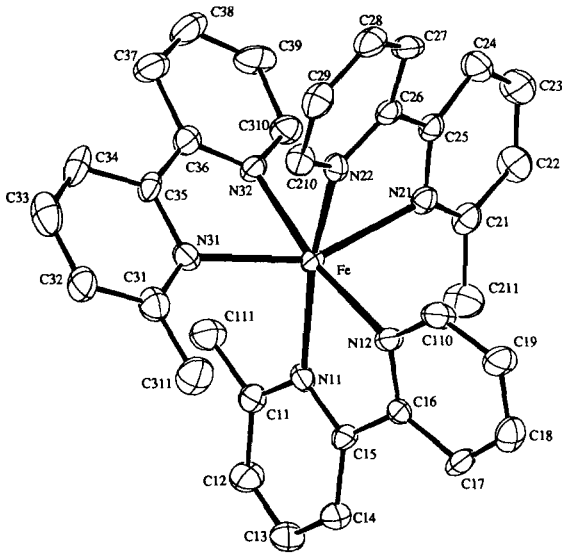

Fig. 8. Structure of $[Fe(mbpy)_3]^{2+}$ showing the atom labelling scheme (hydrogen atoms are omitted for clarity).

tion, similar to that of the tris(2-methyl-1,10-phenanthroline)iron(II) cation [7], presumably because this configuration leads to reduced inter-ligand

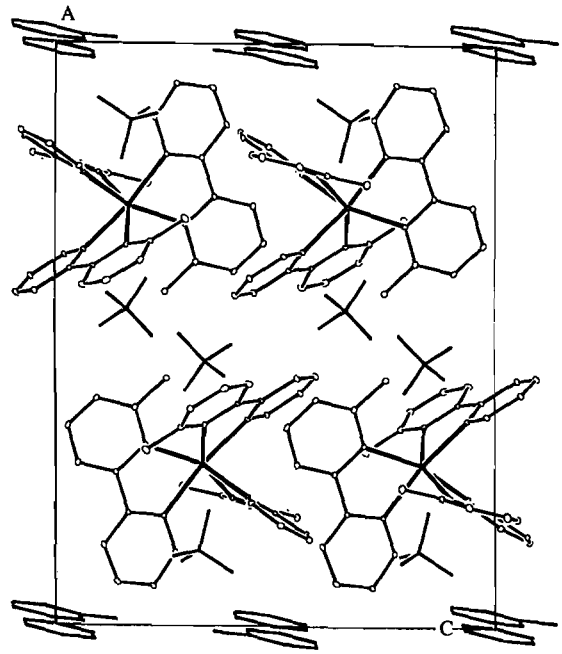

Fig. 9. A view of the unit cell contents for $[Fe(mbpy)_3][ClO_4]_2 \cdot 0.5$mbpy projected down *b*.

TABLE 4. Bond lengths (Å) for $[Fe(mbpy)_3][ClO_4]_2$ with e.s.d.s in parentheses

Fe–N11	2.192(7)	Fe–N12	2.197(7)	Fe–N21	2.259(7)	Fe–N22	2.157(7)
Fe–N31	2.243(7)	Fe–N32	2.204(7)	N11–C11	1.369(11)	N11–C15	1.362(10)
N12–C16	1.323(10)	N12–C110	1.339(11)	N21–C21	1.324(10)	N21–C25	1.341(10)
N22–C26	1.336(10)	N22–C210	1.346(11)	N31–C31	1.321(11)	N31–C35	1.380(10)
N32–C36	1.314(10)	N32–C310	1.357(10)	C11–C12	1.388(12)	C11–C111	1.471(12)
C12–C13	1.366(13)	C13–C14	1.378(14)	C14–C15	1.368(11)	C15–C16	1.465(12)
C16–C17	1.404(12)	C17–C18	1.384(13)	C18–C19	1.352(13)	C19–C110	1.384(12)
C21–C22	1.381(13)	C21–C211	1.473(13)	C22–C23	1.385(14)	C23–C24	1.375(14)
C24–C25	1.395(12)	C25–C26	1.495(12)	C26–C27	1.389(12)	C27–C28	1.375(13)
C28–C29	1.378(14)	C29–C210	1.370(13)	C31–C32	1.405(13)	C31–C311	1.435(13)
C32–C33	1.359(15)	C33–C34	1.390(15)	C34–C35	1.407(13)	C35–C36	1.443(12)
C36–C37	1.433(12)	C37–C38	1.355(15)	C38–C39	1.371(15)	C39–C310	1.384(12)
Cl1–O11	1.363(3)	Cl1–O12	1.363(3)	Cl1–O13	1.363(3)	Cl1–O14	1.363(3)
N41–C41	1.331(12)	N41–C45	1.327(11)	C41–C42	1.390(12)	C41–C411	1.459(1)
C42–C43	1.359(14)	C43–C44	1.405(14)	C44–C45	1.393(12)	C45–C46	1.499(18)

TABLE 5. Selected bond angles (°) for $[Fe(mbpy)_3][ClO_4]_2$ with e.s.d.s in parentheses

N11–Fe–N12	74.4(3)	N11–Fe–N21	109.0(3)	N11–Fe–N22	162.0(3)
N11–Fe–N31	95.5(3)	N11–Fe–N32	111.1(3)	N12–Fe–N21	86.9(2)
N12–Fe–N22	88.3(3)	N12–Fe–N31	113.8(3)	N12–Fe–N32	170.1(3)
N21–Fe–N22	74.5(3)	N21–Fe–N31	151.8(3)	N21–Fe–N32	83.5(3)
N22–Fe–N31	86.7(3)	N22–Fe–N32	86.7(3)	N31–Fe–N32	74.5(3)
Fe–N11–C11	126.4(6)	Fe–N11–C15	115.7(6)	C11–N11–C15	117.6(8)
Fe–N12–C16	116.4(6)	Fe–N12–C110	125.4(6)	C16–N12–C110	116.6(8)
Fe–N21–C21	126.8(7)	Fe–N21–C25	111.3(6)	C21–N21–C25	118.7(8)
Fe–N22–C26	117.2(6)	Fe–N22–C210	125.1(7)	C26–N22–C210	117.7(8)
Fe–N31–C31	126.2(7)	Fe–N31–C35	110.5(6)	C31–N31–C35	122.0(9)
Fe–N32–C36	115.1(7)	Fe–N32–C310	125.9(6)	C36–N32–C310	117.8(8)

TABLE 6. Fractional coordinates for non-hydrogen atoms in $[Fe(mbpy)_3][ClO_4]_2 \cdot 0.5mbpy$

Fe	0.72250(6)	0.04098(9)	0.16514(7)	N11	0.6904(4)	−0.0108(5)	0.2963(5)
N12	0.8117(4)	0.0579(6)	0.2530(4)	N21	0.7790(4)	−0.0858(6)	0.0980(5)
N22	0.7792(3)	0.1125(6)	0.0611(5)	N31	0.6553(4)	0.1780(6)	0.1610(5)
N32	0.6447(4)	0.0082(6)	0.0625(5)	C11	0.6261(6)	−0.0378(7)	0.3193(6)
C12	0.6107(5)	−0.0607(8)	0.4067(7)	C13	0.6584(7)	−0.0502(9)	0.4729(7)
C14	0.7226(6)	−0.0209(8)	0.4497(6)	C15	0.7380(5)	−0.0044(6)	0.3626(6)
C16	0.8065(5)	0.0206(6)	0.3343(6)	C17	0.8629(6)	0.0044(7)	0.3905(6)
C18	0.9261(6)	0.0303(8)	0.3594(8)	C19	0.9326(5)	0.0702(9)	0.2772(7)
C110	0.8740(6)	0.0822(8)	0.2266(6)	C111	0.5747(5)	−0.0455(9)	0.2478(6)
C21	0.7773(5)	−0.1834(8)	0.1187(7)	C22	0.7921(6)	−0.2574(8)	0.0570(8)
C23	0.8075(7)	−0.2290(10)	−0.0289(8)	C24	0.8118(5)	−0.1281(9)	−0.0514(7)
C25	0.7979(4)	−0.0590(7)	0.0161(7)	C26	0.8052(4)	0.0521(8)	−0.0008(6)
C27	0.8409(5)	0.0891(9)	−0.0727(6)	C28	0.8503(5)	0.1921(10)	−0.0784(7)
C29	0.8263(5)	0.2556(8)	−0.0134(8)	C210	0.7891(5)	0.2131(8)	0.0529(6)
C211	0.7615(6)	−0.2143(8)	0.2100(7)	C31	0.6597(5)	0.2576(9)	0.2141(7)
C32	0.6277(6)	0.3496(8)	0.1920(8)	C33	0.5921(6)	0.3550(9)	0.1140(10)
C34	0.5837(5)	0.2702(10)	0.0601(8)	C35	0.6172(4)	0.1795(8)	0.0833(7)
C36	0.6124(5)	0.0880(9)	0.0310(6)	C37	0.5732(6)	0.0857(11)	−0.0500(7)
C38	0.5689(6)	−0.0047(12)	−0.0926(8)	C39	0.5982(6)	−0.0910(10)	−0.0587(7)
C310	0.6364(5)	−0.0811(8)	0.0188(6)	C311	0.6999(6)	0.2502(8)	0.2942(8)
Cl1	0.8700(1)	0.0195(2)	0.6727(2)	O11	0.9069(3)	0.0035(5)	0.5983(3)
O12	0.8805(4)	−0.0583(4)	0.7310(4)	O13	0.8896(4)	0.1085(4)	0.7115(4)
O14	0.8030(2)	0.0245(6)	0.6501(4)	Cl2	0.4552(4)	0.1661(5)	0.3403(6)
O21	0.4292(9)	0.2470(8)	0.3847(11)	O22	0.4852(6)	0.1013(9)	0.3996(7)
O23	0.4043(6)	0.1169(11)	0.2956(10)	O24	0.5019(7)	0.1991(13)	0.2814(9)
Cl2′	0.4548(8)	0.1750(9)	0.3272(10)	O21′	0.4202(18)	0.2217(15)	0.3933(18)
O22′	0.5222(9)	0.1945(24)	0.3377(22)	O23′	0.4441(13)	0.0730(9)	0.3312(14)
O24′	0.4328(16)	0.2109(19)	0.2468(15)	N41	1.0064(5)	0.0980(9)	1.0632(9)
N42	1.0059(5)	−0.1259(10)	0.9287(9)	C41	1.0158(5)	0.1976(9)	1.0573(10)
C42	1.0310(5)	0.2458(11)	0.9779(9)	C43	1.0363(5)	0.1868(11)	0.9043(11)
C44	1.0268(5)	0.0813(11)	0.9071(10)	C45	1.0117(5)	0.0419(9)	0.9903(10)
C46	1.0006(5)	−0.0698(12)	1.0015(10)	C47	0.9855(5)	−0.1093(11)	1.0847(10)
C48	0.9760(5)	−0.2148(12)	1.0875(11)	C49	0.9813(5)	−0.2737(11)	1.0139(9)
C410	0.9965(6)	−0.2256(11)	0.9345(11)	C411	1.0098(6)	0.2589(12)	1.1376(11)

interactions. In $[Fe(mbpy)_3]^{2+}$ these are reduced further by the ligands adopting conformations twisted about the intra-ligand C–C bridge. The angles between the normals of planes 1 and 2, of planes 3 and 4, and of planes 5 and 6 are 16.4, 17.8 and 4.3°, severally (planes 1 to 6 are the best least-squares planes for the pyridyl rings containing atoms N11, N12, N21, N22, N31, N32, severally; the maximum deviation of an atom from these planes is 0.05 Å). The tilting of the two rings of each ligand molecule is thus very significant and much more pronounced than in the comparable complexes of unsubstituted bipyridine. Although each pyridyl ring is essentially planar the iron atom is, in all instances except for plane 4, considerably displaced from these planes, the respective distances being 0.26, 0.49, 0.78, 0.02, 0.56 and 0.53 Å. This obviously must result in a weakening of the metal–nitrogen interaction and thus contribute to the accessibility of the quintet state for iron(II) in this system. The situation is similar, though less extreme, to that in the tris(3,3′-dimethylbipyridine)iron(II) complex where the metal atom lies approximately 0.6 Å out of the coordination plane of all the donor atoms [10]. A steric barrier to coordination from the methyl group, though present, is not so pronounced in the present system as in the $[Fe(me\text{-}phen)_3]^{2+}$ complex. Thus while the average Fe–N distance (2.21 Å) is virtually the same for the two systems, the differences in the $Fe–N_{C–Me}$ and $Fe–N_{C–H}$ distances are not so marked in $[Fe(mbpy)_3]^{2+}$, the average values being 2.23 and 2.19 Å, respectively. Surprisingly, for ligand 1 the $Fe–N_{C–Me}$ and $Fe–N_{C–H}$ distances are almost the same, the former being apparently slightly shorter in fact.

The actual coordination environment about the metal atom is considerably distorted from regular octahedral, the Fe–N distances varying from 2.157(7)–2.259(7) Å and the N–Fe–N angles deviating from 90° by as much as 15.6°. Consideration of the trigonal twist angles which are relevant to the stereochemistry of tris(bidentate)metal chelates shows that the actual triangular faces are considerably distorted and thus a single value for the twist angle

does not apply. The average value found for the present system is 48.2°, which compares with the value 48.8° calculated in the same way for $[Fe(mephen)_3]^{2+}$. The value in both instances is greater than that predicted from the empirical relationship derived by Kepert [34] between the normalised bite of the ligand and the twist angle. Deviation is generally observed in complexes of bipyridine or phenanthroline and is associated with inter-ligand interactions involving the α-hydrogen atoms [35], strengthened in the methyl-substituted ligands by the increased bulk of the substituent.

The uncoordinated ligand molecules are not associated with the anions and are present merely as clathrated species. Their structure is unremarkable, the molecules being planar with the two nitrogen atoms in a *trans* configuration, as they are in free, unsubstituted bipyridine [36]. Bond lengths and angles in the free molecules of 1 and bipyridine are very similar. The free ligand is disordered across a centre of symmetry so both halves of the molecule have the same internal ring coordinates. This disorder leads to a variety of environments and it is not surprising that as a consequence one of the two perchlorate ions is orientationally disordered with relative occupancies of 63 and 37% for the two orientations. The bond lengths within the free ligand differ little from those in the coordinated, although a small decrease in the inter-ring bridge is evident, as it generally is in complexes of unsubstituted bipyridine. The bond lengths and angles within each anion are normal. The occurrence of two anionic sites may be expected to impose two different lattice contributions to the quadrupole splitting in the Mössbauer spectrum and account for the line broadening observed at low temperatures, as discussed earlier.

It is obvious that the methyl substituent exerts a strong steric effect in the complex, this appearing both as an inter-ligand repulsion and as a barrier to close approach of the metal atom. These interactions are no doubt primarily responsible for the highly distorted nature of the metal ion environment and this distortion in turn contributes to the accessibility of the quintet state for iron(II) [37].

Supplementary Material

Structure factor tables, positional and thermal parameters for all atoms, as well as all bond distances, bond angles and torsional angles and analytical data for the complexes are available from the authors.

Acknowledgements

D.O. is grateful for an Australian Development Assistance Bureau Award. Appreciation is expressed to Dr P. Pham for the microanalytical data and to Mr D.C. Craig, University of New South Wales, for the collection of the diffraction data. Financial support from the Australian Research Council is gratefully acknowledged.

References

1 H. Irving and D. H. Mellor, *J. Chem. Soc.*, (1962) 5237.
2 H. A. Goodwin and R. N. Sylva, *Aust. J. Chem., 21* (1968) 83.
3 E. König, G. Ritter, H. Spiering, S. Kremer, K. Madeja and A. Rosenkranz, *J. Chem. Phys., 56* (1972) 3139.
4 E. König, G. Ritter, B. Braunecker, K. Madeja, H. A. Goodwin and F. E. Smith, *Ber. Bunsenges. Phys. Chem., 76* (1972) 393.
5 J. Fleisch, P. Gütlich, K. M. Hasselbach and W. Müller, *Inorg. Chem., 15* (1976) 958.
6 E. König, G. Ritter and H. A. Goodwin, *J. Inorg. Nucl. Chem., 39* (1977) 1773.
7 H. A. Goodwin, E. S. Kucharski and A. H. White, *Aust. J. Chem., 36* (1983) 1115.
8 L. Johansson, M. Molund and A. Oskarsson, *Inorg. Chim. Acta, 31* (1978) 117.
9 E. König, *Prog. Inorg. Chem., 35* (1987) 527.
10 D. C. Craig, H. A. Goodwin and D. Onggo, *Aust. J. Chem., 41* (1988) 1157.
11 C. M. Harris, S. Kokot, H. R. H. Patil, E. Sinn and H. Wong, *Aust. J. Chem., 25* (1972) 1631.
12 E. J. Halbert, C. M. Harris, E. Sinn and G. J. Sutton, *Aust. J. Chem., 26* (1973) 951.
13 W. M. Reiff and G. J. Long, *Inorg. Chem., 13* (1974) 2150.
14 J. Fleisch, P. Gütlich and K. M. Hasselbach, *Inorg. Chim. Acta, 17* (1976) 51.
15 K. J. Schmalzl and L. A. Summers, *Aust. J. Chem., 30* (1977) 657.
16 P. Main, *MULTAN80*, University of York, U.K., 1980.
17 A. D. Rae, *RAELS87*, University of New South Wales, Australia, 1987.
18 J. A. Ibers and W. C. Hamilton (eds.), *International Tables for X-ray Crystallography*, Vol. 4, Kynoch Press, Birmingham, U.K., 1974.
19 C. K. Johnson, *ORTEP-II*, Oak Ridge National Laboratory, TN, U.S.A., 1976.
20 D. F. Evans, *J. Chem. Soc.*, (1959) 2003.
21 T. Kaufmann, J. König and A. Woltermann, *Chem. Ber., 109* (1976) 3864.
22 K. T. Potts and P. A. Winslow, *J. Org. Chem., 50* (1985) 5475.
23 T. L. J. Huang and D. G. Brewer, *Can. J. Chem., 59* (1981) 1689.
24 R. H. Fabian, D. M. Klassen and R. W. Sonntag, *Inorg. Chem., 19* (1980) 1977.
25 A. A. Del Paggio and D. R. McMillan, *Inorg. Chem., 22* (1983) 691.
26 G. R. Newkome, F. R. Fronczek, V. K. Gupta, W. E. Puckett, D. C. Pantaleo and G. E. Kiefer, *J. Am. Chem. Soc., 104* (1982) 1782.
27 E. König, *Coord. Chem. Rev., 3* (1968) 471.
28 E. König, G. Ritter, S. K. Kulshreshtha and S. M. Nelson, *Inorg. Chem., 21* (1982) 3022.
29 A. T. Baker, H. A. Goodwin and A. D. Rae, *Inorg. Chem., 26* (1987) 3513.
30 P. Stupik, W. M. Reiff, R. Hage, J. Jacobs, J. G. Haasnoot and J. Reedijk, *Hyperfine Interact., 40* (1988) 343.

31 D. M. Klassen, *Inorg. Chem., 15* (1976) 3166.
32 S. M. Hart, J. C. A. Boeyens and R. D. Hancock, *Inorg. Chem., 22* (1983) 982.
33 M. A. Robinson, J. D. Curry and D. H. Busch, *Inorg. Chem., 3* (1963) 1178.
34 D. L. Kepert, *Inorg. Chem., 11* (1972) 1561.
35 H. A. Goodwin, D. L. Kepert, J. M. Patrick, B. W. Skelton and A. H. White, *Aust. J. Chem., 37* (1984) 1817.
36 M. H. Chisholm, J. C. Huffman, I. P. Rothwell, P. G. Bradley, N. Kress and W. H. Woodruff, *J. Am. Chem. Soc., 103* (1981) 4945.
37 E. König and S. Kremer, *Theor. Chim. Acta, 20* (1971) 143.